

Determining the Residual Stresses of Circular Weld Bead with Eigenstrain BIE as an Inverse Approach

* H. Ma¹, Y.J. Tang², and C. Yan³

¹College of Sciences, Shanghai University, Shanghai 200444, China.

²Shanghai Institute of Applied Mathematics and Mechanics, Shanghai 200072.

³School of Chemistry, Physics and Mechanical Engineering, Queensland University of Technology, QLD 4001, Australia.

*Corresponding author: hangma@staff.shu.edu.cn

Abstract

In the present work, based on the computational model of the eigenstrain boundary integral equations (BIE) as an inverse problem, the algorithm is investigated to determine the circular weld bead induced residual stresses, where the eigenstrain is considered to be the origin of residual stresses in structures. In order to reduce the number of unknowns and to consider the stability of inverse problem, the eigenstrains are approximated in terms of low-order polynomials in the local area, which is divided by cells, around welded zones according to the features of welding. The corresponding domain integrals with polynomial eigenstrains in each cell are transformed into the boundary integrals to preserve the favorable features of the boundary-only discretization in the numerical solutions. The sensitivity matrix in the inverse approach for evaluating the eigenstrain fields represented by the coefficients of polynomials is constructed with the aid of measured stresses in the domain after welding over a few selected measuring points. In the numerical examples, the residual stresses of circular weld beads in both the finite and infinite plates are evaluated with the proposed procedure, verifying the feasibility and effectiveness of the present algorithm.

Keywords: residual stress, circular weld bead, eigenstrain, boundary integral equation, inverse approach

Introduction

The circular weld beads are used quite frequently in the welded structures as well as in the repair weld and in the test pieces for evaluating the effects of stress corrosion cracks, so that the residual stress fields such formed become one of the primary concerns of engineers and researchers in this field. As the residual stresses have a significant influence on the performance of related components in service [Masubuchi (1980)], when such a component is in service, the associated residual stresses may superimpose on the applied stress to influence the deformation behavior of components, which induce distortion during further machining and cause unexpected failure or reduce the service time of components. Since the nature of residual stress is in self-equilibrium, however, its determination is not an easy task, especially with the mechanical techniques [Prime (1999)].

There are a great number of techniques to detect the residual stresses in a solid which can be classified as three major groups: physical, mechanical and numerical techniques. In the physical techniques, for example, the variation of inter-crystal distances can be detected by X-ray diffraction [Korsunsky et al (2006)] or by sound speed changes in acoustoelasticity or by magnetic techniques, most of them depending on certain material properties. In contrast, in the mechanical techniques, since the direct detection is impossible, parts of the material have to be removed from the solid to disturb the stress balance while the response of the specimen is measured in terms of either strains or shape changes at some other locations on the surface of the body. The blind-hole drilling may be the most commonly used residual stress measuring method in practice and consists essentially of drilling a small blind-hole on the surface of solid and measuring the strain field induced by material removal, usually by means of electrical resistance strain gauges. In addition to the use of strain

gauges, the strain fields can also be measured by photo means such as the electronic speckle pattern interferometer [Suterio et al (2006)] or the digital image correlation in recent advances. In addition to the cost of mechanical methods, all of them are more or less destructive to the measured component by material removals due to the nature of self-balancing. It is evident that the mechanical techniques always provide a limited level of detail, due to the finite number of discrete data points that restricts the possibility of reconstructing full-field stress distributions.

Numerical methods present a supplementary but effective means for determining the residual stresses. However, the detailed modeling of the process of residual stress generation requires the knowledge of numerical models for analyzing sophisticated coupled microstructural and thermo-mechanical behaviors, which rely deeply on the understanding of constitutive laws and material parameters. As is widely accepted, residual stresses in components at service are caused by incompatible internal permanent strains, named originally as the inherent strains [Ueda et al (1986); Ma et al (1998a)] and lately as the eigenstrains [Jun et al (2010)], induced by any inhomogeneous inelastic deformation, temperature gradients or phase transformations during manufacturing and processing of the components. By making use of the information observed from the experiment at a number of selected points, the unknown eigenstrain distributions can be retrieved using the finite element method (FEM) [Lee et al] or the boundary element method (BEM) [Cao et al (2002)], following the mathematical framework of the inverse problem of eigenstrain theory to obtain the whole field of residual stresses.

In spite of the inelastic origin of eigenstrains, the inherent state of residual stress fields falls really into elastic regime so that the BEM would be the most efficient numerical means to deal with the residual stress problems [Qian et al (2004; 2005)]. Based on the concept of eigenstrain, a straightforward computational model as an inverse approach was proposed with the eigenstrain formulations of boundary integral equations to determine the welding residual stresses [Ma et al (2012)]. In the present work, the eigenstrains are approximately expressed in terms of low-order polynomials in the local area around the heat affected zones of circular weld beads, which is divided by cells, according to the features of welding. The corresponding domain integrals with polynomial eigenstrains are transformed into the boundary integrals [Ma et al (1998b)] so that the attractive features of the boundary-only discretization are reserved in the process of numerical solutions using the boundary point method (BPM) [Ma et al (2010)]. The sensitivity matrix in the inverse approach for evaluating the eigenstrain fields represented by the coefficients of polynomials is constructed with the aid of measured stresses in the domain after welding over a few selected measuring points. In the numerical examples, the residual stresses of circular weld beads in both the finite and infinite plates are evaluated with the proposed procedure, verifying the feasibility and effectiveness of the present algorithm.

Computational Model

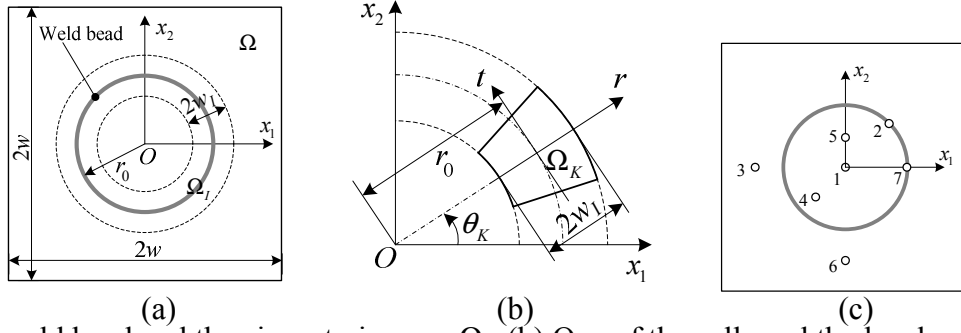
Eigenstrain Boundary Integral Equations

The displacements and the stresses of a weld plate, Ω , in the static state without body force can be described by the eigenstrain boundary integral equations as follows [Ma et al (2012)]:

$$Cu_i(p) + \int_{\Gamma} u_j(q) \tau_{ij}^*(p, q) d\Gamma(q) = \int_{\Gamma} \tau_j(q) u_{ij}^*(p, q) d\Gamma(q) + \int_{\Omega_I} \varepsilon_{jk}^0(q) \sigma_{ijk}^*(p, q) d\Omega(q) \quad (1)$$

$$C\sigma_{ij}(p) = \int_{\Gamma} \tau_k(q) u_{ijk}^*(p, q) d\Gamma(q) - \int_{\Gamma} u_k(q) \tau_{ijk}^*(p, q) d\Gamma(q) + \int_{\Omega_I - \Omega_\varepsilon} \varepsilon_{kl}^0(q) \sigma_{ijkl}^*(p, q) d\Omega(q) + \varepsilon_{kl}^0(p) O_{ijkl}^* \quad (2)$$

where Ω_I ($\Omega_I \in \Omega$) represents the local area having unknown eigenstrains, ε_{ij}^0 , around the weld bead in Ω , since it is generally true that the position of the local area is known a priori in welding. p and q are the source and field points, u_{ij} , τ_{ij} , and σ_{ij} represent the fundamental solutions for displacement, traction and stress, respectively. u_{ijk} , τ_{ijk} and σ_{ijk} are the related derivatives. C is the conventional boundary shape coefficient, $C=1/2$ if p is on the smooth boundary Γ . Ω_ε is a small region of radius ε around point p when $p \in \Omega_I$, and O_{ijkl}^* is the corresponding free term resulted from the domain integral in (2) which can be derived using the conventional limiting techniques with a small ε region since the kernel of this domain integral is strong singular. A square plate $2w \times 2w$ with a circular weld bead is shown in Fig. 1a.



(a) The weld bead and the eigenstrain zone Ω_j ; (b) One of the cells and the local coordinate for the eigenstrain zone; (c) The position of measuring points

Figure 1. The plate with a circular weld bead

Eigenstrain Representation

It is obvious from (1) and (2) that once the distributions of the eigenstrains ε_{ij}^0 in the domain integrals are known, the unknown boundary displacements can be solved using (1) and the total fields of stresses can be computed using (2). Considering the features of thermal cycles of welding, the distributions of eigenstrains can be approximately expressed in terms of low-order polynomials in the local area Ω_j :

$$\varepsilon_{ij}^0 = \sum_{m=0, n=0}^{m+n=M} \alpha_{ij}^{mn} x_1^m(q) x_2^n(q) \quad (3)$$

where M is the number of terms of polynomials and α_{ij}^{mn} the coefficients to be identified. m and n are integers. In fusion welding, the eigenstrain distributions can be expected to be smooth since the temperature field in welding can be expressed by smooth functions especially during the cooling stage. Owing to the similar reason, the eigenstrain can be assumed to be zero at the boundary of the eigenstrain domain. The polynomial representations (3) for eigenstrain are inherently smooth, giving a smooth constraint on the eigenstrain field. The domain integrals with polynomial eigenstrains in (1) and (2) can be transformed into the boundary integrals by introducing the two-point variables

$$x_i = x_i(q) - x_i(p) \quad (4)$$

With this definition, the domain integrals with certain term of polynomials in (1) and (2), respectively, can be expressed in the form of the two-point polynomials as follows:

$$\begin{aligned} & \alpha_{kl}^{mn} \left\{ \int_{\Omega_j} x_1^m(q) x_2^n(q) \sigma_{ijk}^* d\Omega \right\} \\ &= \alpha_{kl}^{mn} \left\{ \sum_{s=0}^m \sum_{t=0}^n \frac{m!n!}{(m-s)!s!(n-t)!t!} [x_1(p)]^{m-s} [x_2(p)]^{n-t} \int_{\Omega_j} x_1^s x_2^t \sigma_{ijk}^* d\Omega \right\} \quad (5) \\ & \quad \alpha_{kl}^{mn} \left\{ \int_{\Omega_j - \Omega_\varepsilon} x_1^m(q) x_2^n(q) \sigma_{ijkl}^* d\Omega + x_1^m(p) x_2^n(p) O_{ijkl}^* \right\} \\ &= \alpha_{kl}^{mn} \left\{ \sum_{s=0}^m \sum_{t=0}^n \frac{m!n!}{(m-s)!s!(n-t)!t!} [x_1(p)]^{m-s} [x_2(p)]^{n-t} \times \int_{\Omega_j - \Omega_\varepsilon} x_1^s x_2^t \sigma_{ijkl}^* d\Omega + x_1^m(p) x_2^n(p) O_{ijkl}^* \right\} \quad (6) \end{aligned}$$

where m, n, s and t are all integers. $x_i, x_i(p)$ and $x_i(q)$ are defined in (4). Then the domain integrals at the right hand sides in (5) and (6) with eigenstrains in the form of two-point polynomials can be transformed into the boundary integrals [Ma et al (1998b)], respectively. In this way, the favorable features of the boundary-only discretization are reserved. However, considering the difficulty of representing eigenstrains with low-order polynomials in a ring area formed by the circular weld bead as shown in Fig. 1a and for the purpose of reducing the number of unknown coefficients, the eigenstrain zone is divided into cells in the present work, one of them being shown in Fig. 1b. The low-order polynomials in each cell Ω_k are represented using the local polar coordinates so that all of the polynomials in the cells are the same. That is, the polynomials in each cell have the same number of terms with the same coefficients owing to the circular weld bead. The domain integrals in (1) and (2) become

$$\int_{\Omega_I} \boldsymbol{\varepsilon}_{jk}^0 \boldsymbol{\sigma}_{ijk}^* d\Omega = \sum_{K=1}^{N_I} \int_{\Omega_K} \boldsymbol{\varepsilon}_{jk}^0 \boldsymbol{\sigma}_{ijk}^* d\Omega \quad (7)$$

$$\int_{\Omega_I - \Omega_e} \boldsymbol{\varepsilon}_{kl}^0 \boldsymbol{\sigma}_{ijkl}^* d\Omega = \sum_{K=1}^{N_I} \int_{\Omega_K} \boldsymbol{\varepsilon}_{kl}^0 \boldsymbol{\sigma}_{ijkl}^* d\Omega \quad (8)$$

respectively, where N_I is the number of cells divided and the eigenstrains and the kernels in each Ω_K are also computed in the local polar coordinates.

Inverse Approach

In the inverse approach, the information from experiments is required to identify the unknown coefficients α_{ij}^{mn} in (3), the stresses measured after welding in the domain at a number of selected measuring points, $x^{(k)}$

$$\boldsymbol{\sigma}_{ij}(x^{(k)}) = \boldsymbol{\sigma}_{ij}^{0(k)}, \quad x^{(k)} \in \Omega, k=1,2,\dots, M_S \quad (9)$$

where $\boldsymbol{\sigma}_{ij}^{0(k)}$ is the measured stresses and M_S the number of measuring points of stresses. Since the residual stresses of weld plates have three components, σ_{11} , σ_{12} and σ_{22} , at one point for the two-dimensional problem, the number of known information from experiments is $3M_S$. By employing the BPM [Ma et al (2010)] and noticed the traction-free boundary conditions in the residual stress problem, the displacement equation (1) combined with (7) can be written after discretization in matrix form as

$$\mathbf{H}\mathbf{u} = \mathbf{B}\boldsymbol{\alpha}, \quad \mathbf{B} = \sum_{K=1}^{N_I} \mathbf{T}^K \mathbf{B}^K \quad (10)$$

where \mathbf{u} is the vector of displacements at all the N nodal points on the boundary Γ , $\boldsymbol{\alpha}$ the vector of unknown coefficients, and \mathbf{H} and \mathbf{B} the corresponding coefficient matrices. Similarly, the discrete stress equation (2) combined with (8) can be used to compute the stresses at selected points as follows

$$\boldsymbol{\sigma} = \mathbf{F}\mathbf{u} + \mathbf{D}\boldsymbol{\alpha} = (\mathbf{F}\mathbf{H}^{-1}\mathbf{B} + \mathbf{D})\boldsymbol{\alpha} = \mathbf{S}\boldsymbol{\alpha}, \quad \mathbf{D} = \sum_{K=1}^{N_I} \mathbf{T}_\sigma^K \mathbf{D}^K \quad (11)$$

where \mathbf{S} is the so-called sensitivity matrix, \mathbf{F} and \mathbf{D} the corresponding coefficient matrices. The transformation matrices in (10) and (11) are defined respectively as

$$\mathbf{T}^K = \begin{bmatrix} \cos \theta_K & -\sin \theta_K \\ \sin \theta_K & \cos \theta_K \end{bmatrix}, \quad \mathbf{T}_\sigma^K = \begin{bmatrix} \cos^2 \theta_K & -2 \cos \theta_K \sin \theta_K & \sin^2 \theta_K \\ \cos \theta_K \sin \theta_K & \cos^2 \theta_K - \sin^2 \theta_K & -\cos \theta_K \sin \theta_K \\ \sin^2 \theta_K & 2 \cos \theta_K \sin \theta_K & \cos^2 \theta_K \end{bmatrix} \quad (12)$$

\mathbf{B}^K and \mathbf{D}^K are formed from the kernels of domain integrals in (7) and (8), respectively, which are computed by line integrals after the transformations using (5) and (6). The unknown coefficients of eigenstrains $\boldsymbol{\alpha}$ can be obtained using the least square method by minimizing the object function, Φ , defined as follows

$$\Phi = \frac{1}{2} \|\mathbf{S}\boldsymbol{\alpha} - \boldsymbol{\sigma}^0\|^2 \quad (13)$$

where $\boldsymbol{\sigma}^0$ represents the vector of measured stresses. The unknown eigenstrain coefficients can be computed by the minimizing condition of (8) as $\mathbf{S}^T(\mathbf{S}\boldsymbol{\alpha} - \boldsymbol{\sigma}^0) = 0$ so that to obtain

$$\boldsymbol{\alpha} = (\mathbf{S}^T \mathbf{S})^{-1} \mathbf{S}^T \boldsymbol{\sigma}^0 \quad (14)$$

Numerical Examples

Conditions of Computation

Both the finite and infinite plates with circular weld bead are considered in the numerical examples, corresponding to the cases of test pieces and repair welds, respectively. The finite plate is shown in Fig. 1a with the width of localized area Ω_I being set as $w_I = 0.3w$ expressed in dashed lines where the eigenstrains are distributed. This width is somewhat wider than that of the heat affected zone (HAZ) according to the parameters of the material and welding, since the HAZ refers as to the narrow band with changes in microstructures of the material near fusion line while the eigenstrain domain corresponds to the zone undergoing plastic tensions in cooling stage following compressive

deformations in heating stage in the welding thermal cycle. The boundary Γ is discretized by $N=100$ nodes and the eigenstrain zone Ω_I is divided equally by $N_I=40$ cells, one of them as shown in Fig. 1b, in the application of the BPM.

Only the normal components of eigenstrains in each cell are considered in the analysis and are approximately expressed in terms of low-order polynomials in the polar coordinate as follows

$$\varepsilon_{rr}^0(r) / \varepsilon_S = -4 + 0.78r^2 \quad (15)$$

$$\varepsilon_{\theta\theta}^0(r) / \varepsilon_S = -1 + 0.44r^2 \quad (16)$$

where ε_S stands for the material constant, or the yield strain, defined as the strain when the Von Mises stress reaches the yield strength, σ_S , of the material. The eigenstrains given in (15) and (16) satisfy approximately both the zero condition at the border and the maximum value at the center of Ω_I following the features of welding, which are used to compute the control values of stresses such as the measured stresses. The positions for the stress measuring points are shown in Fig. 1c, where the idealized measuring stresses are computed using the BPM with the values of eigenstrains in (15) and (16). With these idealized data, the residual stress can be reconstructed after solving the eigenstrains using the inverse approach stated above. However, as there are always errors in the experimental measurements, 10% random noises are introduced into the idealized data as follows

$$\sigma_{noise}^0 = (1 \pm 0.1ran)\sigma^0 \quad (17)$$

where *ran* represents the random function varying between 0 and 1. With these noisy data, the residual stress can also be reconstructed after solving the eigenstrains using the inverse approach. For the infinite plates, the solution procedure and all parameters are as the same with those of the finite plates except that there is no outer boundary Γ so that the boundary integrals in (1) and (2) vanish.

Computed Results

In all of the following figures, the stress distributions are shown along the x_1 axis. The computed stresses with the inverse approaches are computed using noisy data of three measuring points. The computed results of the infinite and the finite plates are presented in Figs. 2 and 3, respectively, showing the feasibility and effectiveness of the present algorithm.

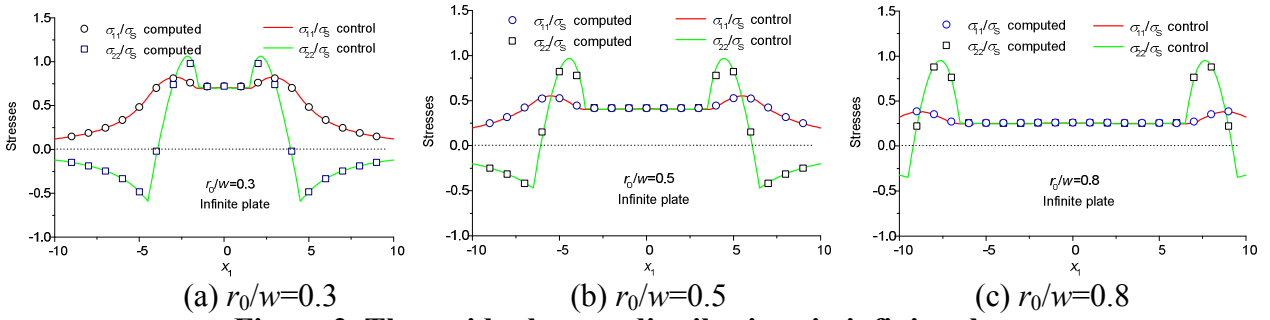


Figure 2. The residual stress distributions in infinite plates

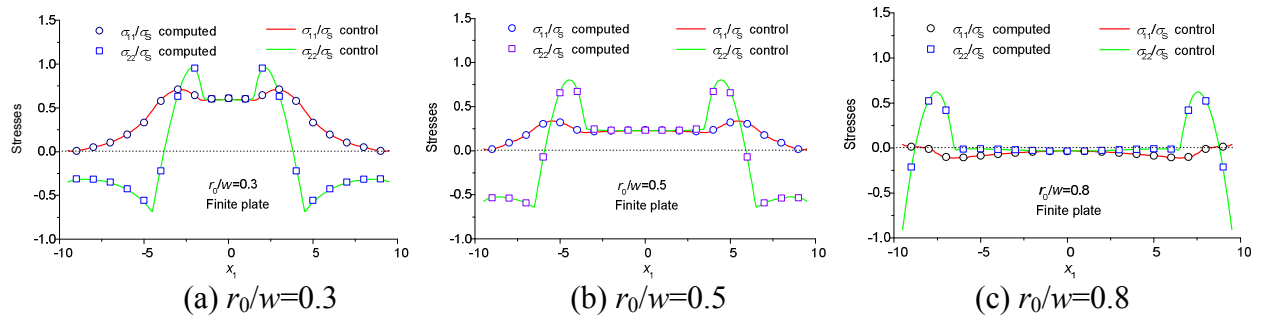


Figure 3. The residual stress distributions in finite plates

It can be seen from Figs. 2 and 3 that there are equally biaxial stress fields ($\sigma_{11}=\sigma_{22}$) inside the circular weld beads. The values of these biaxial stresses decrease with the increase of the radius r_0/w , formed by the constrained shrinkages of the welding plastic zone during cooling stages in both

the transverse and the longitudinal directions, or radius and circular directions respectively in the case of circular weld beads. In general, the transverse shrinkage plays the principal role since the gratitude of it is greater than that of the longitudinal shrinkage so that there are generally the equally tensile biaxial stresses inside the circular weld beads. However, the opposite situation can occur as shown in Fig. 3c that the equally compress biaxial stresses exist when r_0/w is relatively large in the finite plate, since the stress field is formed primarily by the longitudinal shrinkage just like an iron hoop fasten the plate owing to almost the null outer constraint in this case. The longitudinal stresses (σ_{22}) reach the peak values at the weld beads owing to the longitudinal shrinkage.

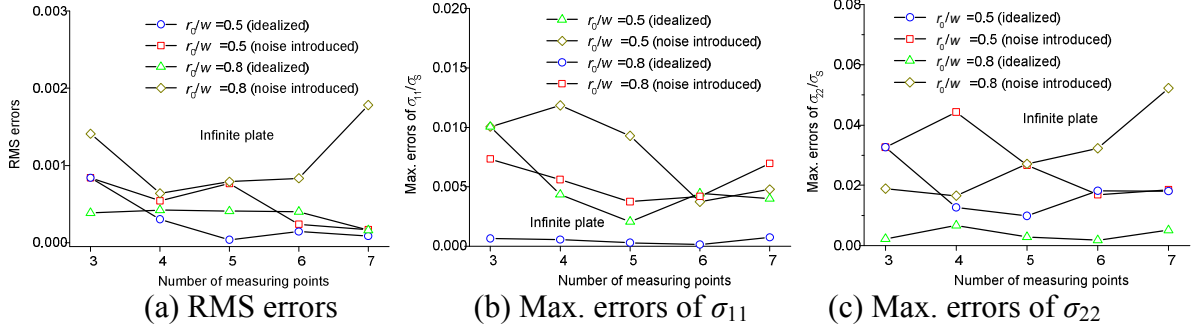


Figure 4. The errors in infinite plates

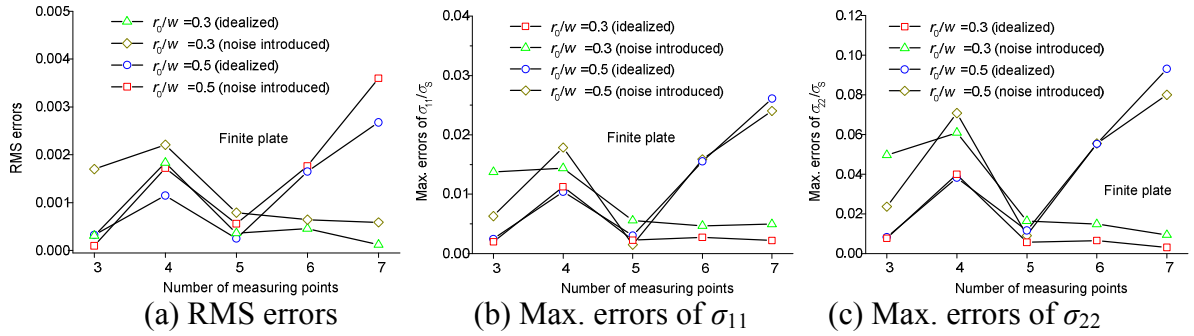


Figure 5. The errors in finite plates

The errors using the idealized and the noise introduced data for the infinite and the finite plates are given in Figs. 4 and 5, respectively, showing that the inverse approach is not too sensitive to the noises in the stress measurement. The residual stress fields can be reconstructed with the proposed approach by using only a small number of selected measuring points, for example, three points 1, 2, and 3 as shown in Fig. 1c, with which the computed stresses are drawn in Fig. 2. The computed results verify the feasibility and effectiveness of the present algorithm.

Conclusions

Using the computational model based on the eigenstrain boundary integral equations (BIE), an algorithm of inverse problem is investigated to determine the circular weld bead induced residual stresses, where the eigenstrain is considered to be the origin of residual stresses in structures. In order to reduce the number of unknowns and to consider the stability of inverse problem, the eigenstrains are approximated by low-order polynomials in the local area, divided into cells, around welded zones according to the features of welding. The sensitivity matrix in the inverse approach for evaluating the eigenstrain fields represented by the coefficients of polynomials is constructed with the aid of measured stresses in the domain after welding over a few selected measuring points. The residual stresses of circular weld beads in both the finite and infinite plates are evaluated in the numerical examples, showing that the proposed inverse approach is not too sensitive to the noises in the stress measurement, verifying the feasibility and effectiveness of the proposed approach.

Acknowledgement: The work was supported by National Natural Science Foundation of China (No.11272195, 11332005, 10972131)

References

- Cao, Y.P., Hu, N., Lu, J., Fukunaga, H., and Yao, Z.H. (2002) An inverse approach for constructing the residual stress field induced by welding, *Journal of Strain Analysis for Engineering Design* **37**, 345-359.
- Jun, T-S., and Korsunsky, A.M. (2010) Evaluation of residual stresses and strains using the eigenstrain reconstruction method, *International Journal of Solids and Structures* **47**, 1678-1686.
- Korsunsky, A.M., Regino, G.M., Latham, D., Liu, J., Nowell, D., and Walsh, M. (2006) Eigenstrain analysis of synchrotron X-ray diffraction measurement of residual strains in machined nickel alloy plates, *Journal of Strain Analysis* **41**, 381-395.
- Lee, C.H. and Chang, K.H. (2008) Three-dimensional finite element simulation of residual stresses in circumferential welds of steel pipe including pipe diameter effects, *Materials Science and Engineering A* **487**, 210-218.
- Ma, H., and Deng, H.L. (1998a) Nondestructive determination of welding residual stresses by boundary element method, *Advances in Engineering Software* **29**, 89-95.
- Ma, H., Kamiya, N., and Xu, S.Q. (1998b) Complete polynomial expansion of domain variables at boundary for two-dimensional elasto-plastic problems, *Engineering Analysis with Boundary Elements* **21**, 271-275.
- Ma, H., Zhou, J., and Qin, Q.H. (2010) Boundary point method for linear elasticity using constant and quadratic moving elements, *Advances in Engineering Software* **41**, 480-488.
- Ma, H., Wang, Y., and Qin, Q.H. (2012) Determination of welding residual stresses by inverse approach with eigenstrain formulations of BIE, *Applicable Analysis* **91**, 807-821.
- Masubuchi, K. (1980) *Analysis of Welded Structures-Residual Stresses, Distortion and Their Consequences*, Pergamon Press, New York.
- Prime, M.B. (1999) Residual stress measurement by successive extension of a slot: the crack compliance method, *Applied Mechanics Review* **52**, 75-96.
- Qian, X.Q., Yao, Z.H., Cao, Y.P., and Lu, J. (2004) An inverse approach for constructing residual stress using BEM, *Engineering Analysis with Boundary Elements* **28**, 205-211.
- Qian, X.Q., Yao, Z.H., Cao, Y.P., and Lu, J. (2005) An inverse approach to construct residual stresses existing in axisymmetric structures using BEM, *Engineering Analysis with Boundary Elements* **29**, 986-999.
- Suterio, R., Albertazzi, A., and Amaral, F.K. (2006) Residual stress measurement using indentation and a radial electronic speckle pattern interferometer-recent progress, *Journal of Strain Analysis* **41**, 515-524.
- Ueda, Y., Jirn, Y., and Yuan, M. (1986) Determination of residual stresses based on the sources of their formation, *Transactions of the Japan Welding Society* **6**, 59-64.